

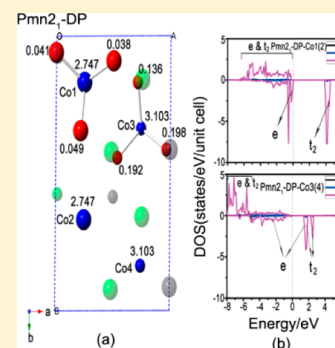
Insights into Changes of Lattice and Electronic Structure Associated with Electrochemistry of $\text{Li}_2\text{CoSiO}_4$ Polymorphs

Caixia Zhang,^{†,‡} Zhenlian Chen,[‡] Yongzhi Zeng,[†] Zhifeng Zhang,[‡] and Jun Li^{*,‡}

[†]College of Physics and Information Engineering, Fuzhou University, Fuzhou 350116, PR China

[‡]Ningbo Institute of Material Technology and Engineering, Chinese Academy of Sciences, Ningbo 315201, PR China

ABSTRACT: First-principles calculations combined with XRD simulations are performed to systematically study crystal structures, bonding characteristics and electronic structures of $\text{Li}_x\text{CoSiO}_4$ ($x = 2.0, 1.5, 1.0$) polymorphs with symmetries $\text{Pmn}2_1\text{-DP}$ and $\text{Pbn}2_1$. The calculated average voltages by lithium extraction agree well with available experiments. CoO_4 tetrahedron is the key structural unit to track the process of delithiation. The oxidation of CoO_4 tetrahedron results in a special pattern of bonding characteristic, which corresponds to spin ordering and may be observable in XRD spectra according to simulation. We find delithiated phases are intrinsic Mott insulators, electronic band gaps change from Mott–Hubbard-type to charge-transfer-type during lithium removing. The swapping of near-gap states is associated with the contraction of the oxidized CoO_4 units, indicating Peierls distortions that may be the physical origin of capacity degrading of Co–silicate chemistry.



1. INTRODUCTION

The urgent need to double energy density from the current state-of-the-art lithium-ion batteries has drawn intense interest in finding or designing a new chemistry beyond oxide cathode materials such as LiCoO_2 and LiMn_2O_4 .^{1–3} High capacity in the desired voltage range of electrolytes with better safety and longer cycle life is continuously the preliminary requirement of the new chemistry for application to scalable energy storage in electric transportation and power-grid.^{4–6} Polyoxyanion compounds, typically, LiFePO_4 proposed by Goodenough, et al, have received wide recognition as safe cathode materials.⁷ Extensive studies on olivine phosphate chemistry have been carried out in order to understand the physical origin of electrochemical performance of polyoxyanion frameworks.^{8–11}

Transition metal silicates Li_2MSiO_4 ($\text{M} = \text{Fe}, \text{Mn}, \text{Co}, \text{Ni}$) have attracted significant attention as a new type of polyoxyanion cathodes since 2005.^{12–19} All cations in Li_2MSiO_4 form tetrahedral units $(\text{XO}_4)^{m-}$ ($\text{X} = \text{Li}, \text{M}, \text{Si}$), very different from octahedral units in olivine phosphate chemistry. All silicate formulas indicate high theoretical capacities over 300 mAh/g if two lithium ions extracted. Fe– and Mn–silicates have achieved nearly 2 Li^+ extraction in recent works,^{20,21} thanks to continuing advances in synthesis of nanostructure and carbon-coating.^{22,23} However, electrochemical performance of Fe– and Mn–silicates seems unstable and their working voltages are low, under 3 V, not preferred with current electrolytes for high energy density. Recent calculations have carefully analyzed the bonding characteristic of $\text{Li}_2\text{FeSiO}_4$ in order to determine the critical structural units that impact electrochemistry of tetrahedral framework.¹⁴ It has been proposed to modify silicate chemistry through synergy effects as did the transition metal ternary oxides.¹⁶ Such an attempt in silicates was mostly limited to the mixing of Fe and Mn, and no improvement was reported in literature so far.²⁴

It is worth pointing out that Co also play a key role in the solid solution ternary oxides, $\text{Li}(\text{NiCoMn})_{1/3}\text{O}_2$ and $\text{Li}(\text{Ni}_{0.8}\text{Co}_{0.15}\text{Al}_{0.05})\text{O}_2$. We notice that Co–silicate could discharge at around 4 V,^{22,23} almost 1 V higher than both Fe– and Mn–silicates and as-prepared Co–silicate polymorphs did not present voltage degradation as always did Fe– and Mn–silicates.^{23,25} However, Co–silicate chemistry is still struggling to deliver high capacity. Therefore, it is important to understand the intrinsic electrochemistry of Co–silicate and its difference from other silicate chemistry. Previous first-principles calculation indicated a high average voltage at 5.0 V would be required to extract fully two lithium ions and average voltages for partially delithiated phases distributed in a wide range for Co–silicate.^{26–28} Those predictions disagreed with recent experiments on carefully characterized Co–silicates with symmetries $\beta_{\text{II}}\text{-Pmn}2_1$, $\beta_1\text{-Pbn}2_1$, and $\gamma_0\text{-P}2_1/n$.^{16,22,23} In our recent work, we identified all the three synthesized polymorphs were in 3D framework lattices, containing no 2D layers existing in Fe– and Mn–silicates, whose crystal structures have been used as the starting template in previous Co–silicate calculations. And the difference of lattice dimensions in Co–silicate polymorphs can be well distinguished by their X-ray diffraction (XRD) spectra.²⁹

This work, mainly by using first-principles calculations and XRD simulations, aims to offer further details on the effect of the crystal structure and electronic structure of Co–silicate $\text{Li}_x\text{CoSiO}_4$ ($x = 2, 1.5, 1.0$) polymorphs on their electrochemical properties. The average voltages are calculated to compare with the available experiment. We find that CoO_4 tetrahedral arrays are a critical structure unit in the process of lithium

Received: January 26, 2014

Revised: March 11, 2014

Published: March 19, 2014

Table 1. Equilibrium Volumes, Total Energies, Magnetic Moments per Co, and Average Voltages for $\text{Li}_x\text{CoSiO}_4$ and Delithiated $\text{Li}_x\text{CoSiO}_4$ ($x = 1.5, 1.0$)^a

	$\text{Li}_2\text{CoSiO}_4$		$\text{Li}_{1.5}\text{CoSiO}_4$		LiCoSiO_4	
	$Pmn2_1$ -DP	$Pbn2_1$	$Pmn2_1$ -DP	$Pbn2_1$	$Pmn2_1$ -DP	$Pbn2_1$
$\Omega(\text{\AA}^3)/\text{formula unit}$	85.095	85.071	86.452	85.093	87.302	87.378
Energy(eV) /formula unit	-51.545	-51.547	-48.564	-48.650	-45.559	-45.539
$m(\mu_B)/\text{Co ion}$	2.759	2.761	2.747, 3.103	2.748, 3.112	3.166	3.166
Voltage-Cal.(V)			4.062	3.896	4.110	4.320
Exp. (V) ^b			3.7–4.0	3.5–4.3	4.0–4.3	4.3–4.6
Others-Cal.(V)					4.4 ^c , 3.4 ^d , 4.13 ^e , 4.1 ^f	

^aAverage voltages for the first 0.5 Li (per formula unit) extraction are from $\text{Li}_2\text{CoSiO}_4$ to $\text{Li}_{1.5}\text{CoSiO}_4$ and the second 0.5 Li (per formula unit) from $\text{Li}_{1.5}\text{CoSiO}_4$ to LiCoSiO_4 , respectively. All calculations are in FM configurations by full GGA+U calculation including structural relaxing. ^bEstimated from ref 23. ^cReference 26. ^dReference 24. ^eReference 28. ^fReference 42. All other calculations were based on layered $Pmn2_1$ structures for one lithium extraction from $\text{Li}_2\text{CoSiO}_4$ to LiCoSiO_4 .

intercalation/extraction. Both atom magnetic moments and local lattice structures of CoO_4 units are investigated for delithiated $\text{Li}_x\text{CoSiO}_4$ ($x = 1.5, 1.0$). The electronic band structures of delithiated phases are found to be intrinsic Mott insulators, changing from Mott–Hubbard-type to charge-transfer-type during delithiation. This may provide physical insights on the limited capacity of Co–silicates. We believe that it is essential to identify the key structural unit that is important to polymorph structure and redox potential for silicate chemistry in general. The understanding of Co–silicate may benefit not only its own electrochemistry but also its use as a potential component in solid solution silicates.

2. COMPUTATIONAL DETAILS

We have determined the key crystal structures of polymorphs: β_{11} - $Pmn2_1$ -DP, β_{11} - $Pbn2_1$, and γ_0 - $P2_1/n$ in our recent work via a detailed comparison with the carefully characterized experimental structures.^{23,30} We have attached DP to β_{11} - $Pmn2_1$ to explicitly indicate its XRD feature and its difference from layered $Pmn2_1$ structures. The primary cell contains 2 formula units for $Pmn2_1$ -DP symmetry and 4 formula units for both $Pbn2_1$ and $P2_1/n$ symmetries. All the three polymorphs are 3D framework lattices, with no 1D lithium ion channel as in LiFePO_4 or 2D lithium ion layers as in LiCoO_2 or Fe– and Mn–silicates. All of them can be distinguished by characters in XRD, $Pmn2_1$ -DP structure shows a double peak around 25° in 2θ while both β_{11} - $Pbn2_1$, and γ_0 - $P2_1/n$ show similar one-triple peak patterns in similar angle ranges. Detailed structure information and comparison with experiment spectra for the fully lithiated $\text{Li}_2\text{CoSiO}_4$ has been reported in our recent work.²⁹ Therefore, this work will focus on partially delithiated $Pmn2_1$ -DP and β_{11} - $Pbn2_1$ to address the key relationship between polymorphic structure and electrochemical properties.

All the calculations were performed using the Vienna ab initio simulation package (VASP)³¹ within the framework of density functional theory (DFT), employing the projector-augmented wave (PAW) method with the spin-polarized generalized gradient approximation (GGA) of Perdew–Burke–Ernzerhof (PBE),^{32–34} and adding the Hubbard parameter correction (GGA+U) to address the strong onsite Coulomb interaction for transition metals. DFT+U method and hybrid functional method are two popular schemes treating the self-interaction error in the conventional DFT framework. But DFT+U method is superior to hybrid functional method in predicting Li intercalation potentials, magnetic moments, and charge localization for all the positive electrode materials containing 3d electrons in transition metals, due to hybrid

functional method being sensitive to the bonding environment of the oxygen, in a way not found in GGA+U.³⁵ Extensive calculations have showed that GGA+U corrections can give quantitatively good agreement with experimental average voltages only through careful adjustment of values of U, which strongly depend on the elements and the valence states in materials.³⁶ For GGA+U calculations, the “effective” value (U–J) was set to be 5.0 eV for $\text{Li}_x\text{CoSiO}_4$ ($x = 2.0, 1.0$), such parameters setting has been considered suitable in previous first-principles studies^{28,36,37} While for $\text{Li}_{1.5}\text{CoSiO}_4$, we found an effective value of 4.5 eV better for describing the formal charge separation between Co^{2+} and Co^{3+} , due to the slight difference of localized d-electrons associated with Co^{2+} and Co^{3+} ions. A 500 eV cut off for the plane-wave basis set was used. Integrations in the first Brillouin zone were performed using Monkhorst-Pack special k -point mesh of $10 \times 12 \times 12$ and $10 \times 6 \times 12$ for the primary unit cells of $\text{Li}_2\text{CoSiO}_4$ polymorphs with symmetries $Pmn2_1$ and $Pbn2_1$, respectively. Structural relaxations were performed with the total energy converged to 10^{-5} eV or better and all forces acting on ions found to be 0.005 eV/Å. The same FM configurations were used to calculate delithiated $\text{Li}_x\text{CoSiO}_4$ as in $\text{Li}_2\text{CoSiO}_4$.

We used the standard first-principles voltage calculation,³⁸ which is derived from the calculated total energies of host compounds

$$\bar{V} = - \frac{E(\text{Li}_x\text{CoSiO}_4) - E(\text{Li}_y\text{CoSiO}_4) - (x - y)\mu(\text{Li})}{(x - y)} \quad (1)$$

where $E(\text{Li}_x\text{CoSiO}_4)$ is the total energy of the initial phase $\text{Li}_x\text{CoSiO}_4$, $E(\text{Li}_y\text{CoSiO}_4)$ is the total energy of the following delithiated phase $\text{Li}_y\text{CoSiO}_4$, $\mu(\text{Li})$ is the total energy of BCC lithium metal, $(x - y)$ is the fraction of extracted lithium ions per formula unit, and \bar{V} is the theoretical average voltage for lithium concentration between x and y , generally used as the intrinsic voltage of electrode materials of Li-ion batteries and compared to experimental voltage measurements in literature. Abundant first-principles calculations over past decade have showed the accuracy and predictive power of this voltage expression (1), often within 0.1–0.2 V of experimental voltage profiles for many cathode materials.^{39–41} For $\text{Li}_{1.5}\text{CoSiO}_4$, we compared two nonequivalent lithium-vacancy configurations for $Pmn2_1$ -DP, and nine nonequivalent configurations for $Pbn2_1$. For LiCoSiO_4 , we considered three nonequivalent distributions for $Pmn2_1$ -DP and 35 representative patterns for $Pbn2_1$. The lithium-vacancy configuration having the lowest energy is used to calculate the voltage profile by eq 1, and then

corresponding delithiated structure is further analyzed to offer insights on the physical origin of electrochemical properties of Co–silicates.

3. RESULTS AND DISCUSSION

3.1. Voltage Profile of $\text{Li}_2\text{CoSiO}_4$ Polymorphs. Table 1 shows that the voltage of $\text{Pmn}2_1$ -DP gently increases from 4.062 to 4.110 V when extracting one full lithium ion per formula unit. On the other hand, the $\text{Pbn}2_1$ structure, while starting from a slightly lower voltage at 3.896 V for the first half Li^+ extraction, jumps to 4.320 V during the second half Li^+ extracting from $\text{Li}_{1.5}\text{CoSiO}_4$ to LiCoSiO_4 . This notable difference of voltage platform changes agrees with the experimental observation.²³ Up to cutoff 4.3 V, about one lithium per formula unit was extracted from $\text{Pmn}2_1$ -DP but only about 0.5 lithium extraction per formula unit for $\text{Pbn}2_1$.²³ To remove one lithium ion from $\text{Pbn}2_1$, cutoff voltage had to be increased to 4.6 V. This confirms a higher voltage platform needed to extract the second half lithium ion from $\text{Pbn}2_1$.

Table 1 also shows previous voltage calculations of partially delithiated phases are distributed in a wide range for Co–silicates,^{24,26,28,42} ranging from 3.4 to 4.4 V and disagreeing with experimental trends. We notice that previous Co–silicate calculations were often using Fe– and Mn–silicates as the starting template, which contains 2D lithium layers.^{24,26–28,42}

As we have pointed out that there exists no such lithium layers in synthesized Co–silicate polymorphs according to XRD analysis.³⁰ Voltage calculations indicate that the electrochemical properties of silicates also strongly depend on detailed tetrahedral networks.⁴³ The dimension of tetrahedral networks is the basic structural difference between Co–silicates and other silicates in synthesized polymorphs. We have found that CoO_4 arrays are a suitable indicator of cationic ordering to track polymorphic structures of Co–silicates in XRD.²⁹ Our calculations of voltage profiles indicate cationic orderings also remarkably affect details of voltage platforms. And our calculation suggests that $\text{Pmn}2_1$ -DP is within the fair voltage window of current electrolytes.

3.2. Spin Ordering Formation with Oxidation of CoO_4 Arrays. Table 1 gives magnetic moments of 2.759 and 2.761 μ_B per Co in $\text{Li}_2\text{CoSiO}_4$ for $\text{Pmn}2_1$ -DP and $\text{Pbn}2_1$, respectively. A clear pattern shows up in magnetic moments with the change of valence states of Co ions during delithiation. All polymorphs confirm the formal valence Co^{2+} with electronic configuration of $3d^7$ at a high-spin state, close to 2.78 μ_B per Co in the same valence Co^{2+} at the high-spin state of the olivine structure LiCoPO_4 .³⁹ However, the Co^{2+} ion in $\text{Li}_2\text{CoSiO}_4$ is in tetrahedral coordination with surrounding weak oxygen ligand field. The quasi-tetrahedral crystal field in $\text{Li}_2\text{CoSiO}_4$ splits the 5-fold degenerated states of the Co ion into two subsets, two low-lying e states and three high-lying t_2 states, different from the order (t_{2g} , e_g) in the strong octahedral ligand field of the olivine structures.

The redox pair $\text{Co}^{2+}/\text{Co}^{3+}$ is conceptually believed important to electrochemistry of Co–silicates. As pointed out in a recent work,⁴⁴ magnetic orders are measurably preferred to the concept of charge-on-ions for the formal valences in the solid state. Table 1 confirms such a clear correlation between the spin states and the formal valences of Co ions in the course of oxidation. It is of interest that the magnetic moment 3.166 μ_B of the tetrahedral Co^{3+} in LiCoSiO_4 is again comparable to 3.27 μ_B of the octahedral Co^{3+} in olivine phosphate.³⁹ Delithiated $\text{Li}_{1.5}\text{CoSiO}_4$ consists of half Co in the formal double and triple

valences, respectively, as manifested by two types of magnetic moments, or formally called the charge separation of Co ions on the CoO_4 arrays. Parts a and b of Figure 1 show a detail

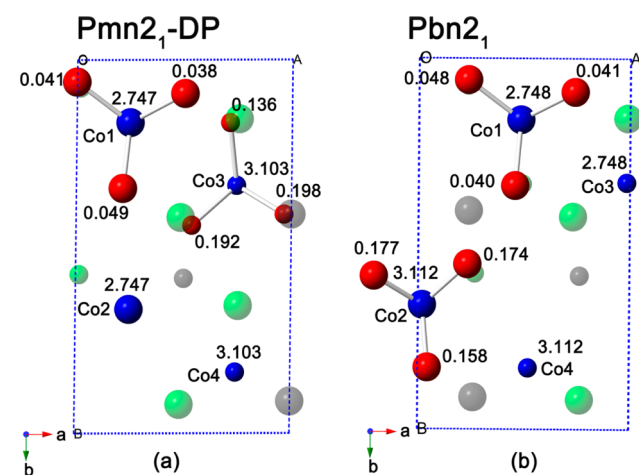


Figure 1. Layout of the spin ordering in delithiated $\text{Li}_{1.5}\text{CoSiO}_4$: (a) $\text{Pmn}2_1$ -DP; (b) $\text{Pbn}2_1$. Green, blue, gray, and red balls correspond to Li, Co, Si, and O atoms with big balls on top layer and small balls on low layer for comparison, with not all ions shown. Magnetic moments are showed in units of μ_B .

pattern of the spin ordering (or magnetic ordering) for β_{II} and β_I $\text{Li}_{1.5}\text{CoSiO}_4$, respectively. In Figure 1a, different spin Co ions settle on different layers; in Figure 1b, both lay on the same layers. We find that the formal valence agrees with the local oxidation situation of CoO_4 arrays. The Co^{3+} ions with 3.1 μ_B are nearby the Li-vacancy while the Co^{2+} ions with 2.7 μ_B locate distant from the Li-vacancy, confirming the formal charge of Co ions. Correspondingly, the magnetic moments of O ions split according to the oxidation states of nearby Co ions: in the range of 0.03–0.07 μ_B if near Co^{2+} ions and increasing to 0.10–0.20 μ_B if near Co^{3+} ions. Thus, tetrahedral CoO_4 as a group is better to track the oxidation/reduction process than does single Co ion.

Table 1 shows that the volume difference between β_{II} and β_I become large at $\text{Li}_{1.5}\text{CoSiO}_4$ but become small at LiCoSiO_4 . $\text{Pmn}2_1$ -DP presents a smooth volume expansion over the entire extraction while $\text{Pbn}2_1$ shows a steep expansion from $\text{Li}_{1.5}\text{CoSiO}_4$ to LiCoSiO_4 , which also accompanies the voltage jump. This is correlating to the different pattern of charge separation that increases Coulomb repulsions among ionic tetrahedrons by the oxidation of Co^{2+} to Co^{3+} ions. Table 2 reveals a clear evolution of bonding characteristic over the entire oxidation from $\text{Li}_2\text{CoSiO}_4$ to LiCoSiO_4 . Overall, the average Si–O bond lengths and SiO_4 tetrahedral volumes remain almost unchanged, indicating a strong covalent bonding between Si and O atoms that plays a central role to keep the structural skeleton stable during lithium extraction. The average Li–O bond lengths show a slight change of about 1% and LiO_4 tetrahedral volumes change less than 2.5%.

Table 2 shows a 20% volume difference between Co^{3+}O_4 and Co^{2+}O_4 , in according with about 7% difference in average Co–O bond lengths. The oxidation of Co^{2+}O_4 to Co^{3+}O_4 units, however, decreases electronic repulsions between Co and the surrounding O ions, mostly due to the transfer of electrons on one e orbitals; consequently, the bond length between Co and O sites becomes reduced. The Co ions in the CoO_4 units with shorter average Co–O bond lengths have higher magnetic

Table 2. Variations of Average Bond Lengths (Li–O, Co–O, Si–O) and Tetrahedral Volumes (LiO₄, CoO₄, SiO₄) upon One Lithium Extraction from Li₂CoSiO₄, through Li_{1.5}CoSiO₄, to LiCoSiO₄ for *Pmn*2₁-DP and *Pbn*2₁ Structures

Li _x CoSiO ₄	<i>Pmn</i> 2 ₁ -DP			<i>Pbn</i> 2 ₁		
	<i>x</i> = 2	<i>x</i> = 1.5	<i>x</i> = 1	<i>x</i> = 2	<i>x</i> = 1.5	<i>x</i> = 1
<i>d</i> _{Co–O} (Å)	1.995	1.993	1.870	1.997	2.006	1.871
		1.870			1.872	
<i>d</i> _{Si–O} (Å)	1.657	1.655	1.648	1.657	1.654	1.649
<i>d</i> _{Li–O} (Å)	2.004	2.026	2.023	2.003	2.005	2.023
<i>V</i> _{CoO₄} (Å ³)	4.064	4.022	3.296	4.075	4.127	3.328
		3.294			3.302	
<i>V</i> _{SiO₄} (Å ³)	2.332	2.320	2.295	2.332	2.321	2.296
<i>V</i> _{LiO₄} (Å ³)	4.094	4.190	4.116	4.086	4.064	4.034

moments at about 3.1 μ_B , while those in the CoO₄ units with longer average Co–O bond lengths have lower magnetic moments at about 2.7 μ_B (cf. Figure 1), in compliance with the inverse dependence of valence states of transitional metal M on average M–O bond lengths.⁴⁵ In *Pmn*2₁-DP, the Co²⁺O₄ unit in Li_{1.5}CoSiO₄ contract slightly from that of Li₂CoSiO₄ while it is a slight expansion in *Pbn*2₁.

There is a concern on whether or not such a theoretical picture of spin ordering (or charge separation) of CoO₄ arrays can be observed.³⁸ Figure 2 predicts the bonding characteristic associated with the oxidation indeed produces visible features in simulated XRD spectra. An obvious splitting of the main peaks shows up in the spectra of Li_{1.5}CoSiO₄, and due to the significant contraction of tetrahedral Co³⁺O₄ units, a set of peaks between 25° and 30° in Figure 2 disappear or combine into a new one around 27° at LiCoSiO₄. Such a spectral observance should confirm the fine effect of oxidation on the CoO₄ tetrahedral bonding network.

3.3. Effects of Electronic Localization. Expanding lattices with shrinking CoO₄ units would prompt one to expect a large space for lithium ion movement, which might suggest a better rate capability and easy discharging for lithium move-in.

However, all synthesized polymorphs of Li₂CoSiO₄ presented awkward discharging capacity even right after the first charging.²³ Hard electron transport has been blamed for the bad discharging. However, the nature of the electronic structures at delithiated phases (*x* = 1.5, 1.0) and the influence of the lattice change on the electron configuration upon the CoO₄ oxidation have not been addressed in details so far.

Our GGA+U calculations find both delithiated phases (*x* = 1.5, 1.0) are Mott insulators for both β_{II} - and β_I -polymorphs and the nature of insulating gaps strongly depends on the oxidation states of Co ions. Parts a and b of Figure 3 show that

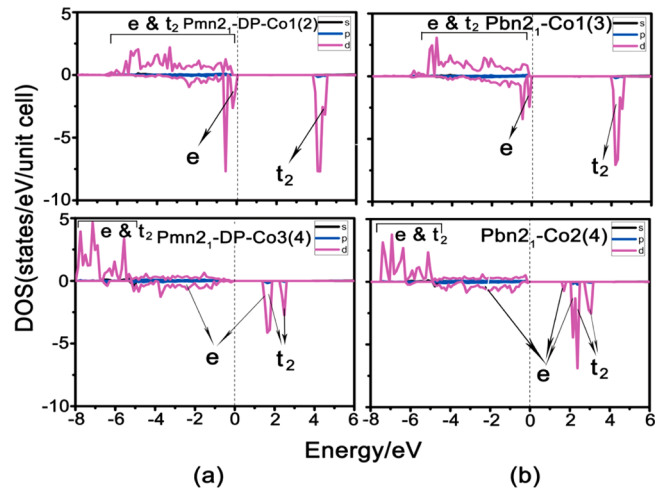


Figure 3. The partial density of states of Co ions on different tetrahedral CoO₄ sites (c. f. Figure 1) in delithiated Li_{1.5}CoSiO₄: (a) *Pmn*2₁-DP; (b) *Pbn*2₁. Fermi levels are at zero.

gap states are similar for β_{II} - and β_I -Li_{1.5}CoSiO₄. *Pbn*2₁ has a slightly bigger gap than *Pmn*2₁. The density of states (DOS) of Co²⁺ in the upper panel of Figure 3 indicates a Mott–Hubbard-type insulating gap between sharp e- and t₂-bands for the electronic configuration e⁴t₂³. The occupied spin-up bands of Co³⁺ ions move −5 eV below Fermi levels, showed in the lower

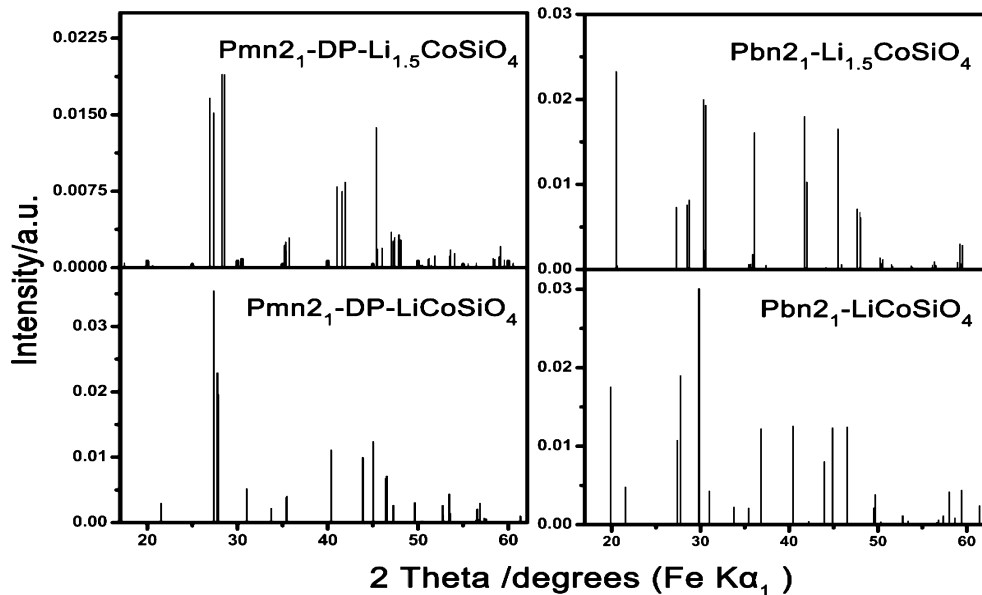


Figure 2. Simulated X-ray diffraction for Li_{1.5}CoSiO₄ and LiCoSiO₄: *Pmn*2₁-DP and *Pbn*2₁.

panel of Figure 3. Because of the strong hybridization, a remarkable change in the Co(3d)-O(2p) orbital overlap (so-called rebonding shift) enhances the covalent bonding between the Co ions and the surrounding oxygen ligands. No obvious sharp occupied spin-down e-bands near the gap presents in the DOS of Co^{3+} , thus, it is a charge-transfer-type insulating. In LiCoSiO_4 , all the formal triple valence Co^{3+} ions are in the configuration $e^3t_2^3$ and the insulating gap becomes a complete charge transfer-type. The swapping of the interaction between 3d(Co)-2p(O) orbitals changes the nature of the insulating gap from Mott-Hubbard-type to charge-transfer-type, a similar phenomenon has been observed in other systems.⁴⁶ This swapping is an evident proof of the band structure change by lithium intercalation/extraction, which is different from simple energy level shift in rigid-band model or redox couple pinning.⁸

The swapping of near-gap states correlates with the contraction of the oxidized CoO_4 units, establishing the cationic electrostatic polarization.¹³ The correlation can be elucidated through a process of tracking how the electronic structure changes along the structural relaxation after removing the lithium ions. Figure 4a shows that $\text{Pmn}2_1$ -DP DOS is a

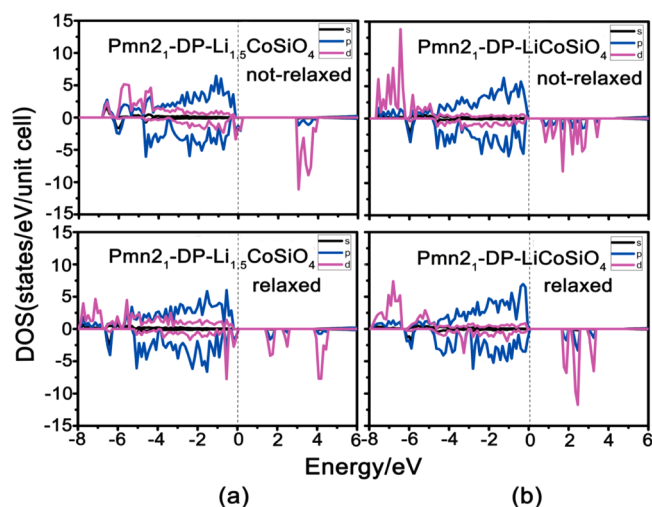


Figure 4. Partial density of states (DOS) of delithiated: (a) $\text{Li}_{1.5}\text{CoSiO}_4$; (b) LiCoSiO_4 . The upper is for nonrelaxed structures, with the lower for well-relaxed structures and only shown for $\text{Pmn}2_1$ -DP. Fermi levels are at zero.

metal-like before lattice relaxation, a clear gap-opening occurs after relaxing the structure of $\text{Li}_{1.5}\text{CoSiO}_4$, along with the building-up of spin ordering by the oxidation of CoO_4 arrays. Figure 4b also shows the gap increasing after relaxing LiCoSiO_4 . Similar gap increasing presents in $\text{Pbn}2_1$, too. For $\text{Li}_{1.5}\text{CoSiO}_4$, the gap of $\text{Pmn}2_1$ -DP opens from 0 to 1.3 eV, larger than the gap increase of $\text{Pbn}2_1$ from 0.6 to 1.5 eV; for LiCoSiO_4 , the gap increase of $\text{Pmn}2_1$ -DP from 0.6 to 1.5 eV is smaller than that of $\text{Pbn}2_1$ from 0.2 to 1.6 eV.

The coexistence of both lattice distortion and band gap opening/increases demonstrates the occurring of Peierls distortions in both delithiated $\text{Li}_{1.5}\text{CoSiO}_4$ and LiCoSiO_4 , which are intrinsic Mott insulators. The resulting electronic localization with gap increases is the physical origin of difficult electronic transport during charging and discharging, which may account for the significant loss in discharging capacity of Co-silicates.

4. CONCLUSION

In this work, we combine first-principles calculations with XRD simulations to systematically study the crystal structures, bonding characteristics and local electronic structures of $\text{Li}_x\text{CoSiO}_4$ ($x = 2.0, 1.5, 1.0$) polymorphs with space groups $\text{Pmn}2_1$ -DP and $\text{Pbn}2_1$. Average voltages by lithium extraction from $\text{Li}_2\text{CoSiO}_4$, through $\text{Li}_{1.5}\text{CoSiO}_4$ to LiCoSiO_4 are calculated, agreeing well with available experiment. The tetrahedron bonding network forms a special pattern in the lattices of $\text{Li}_{1.5}\text{CoSiO}_4$, indicating the formation of spin ordering of CoO_4 arrays, and may be observable in XRD spectra according to simulation. Ordering of CoO_4 arrays can be used to characterize the redox process during lithium ions extraction/intercalation. Both delithiated $\text{Li}_{1.5}\text{CoSiO}_4$ and LiCoSiO_4 are intrinsic Mott insulators. The swapping of the interaction between 3d(Co)-2p(O) orbitals changes electronic band structures from Mott-Hubbard-type to charge-transfer-type, which correlates with the contraction of the oxidized CoO_4 units, demonstrating the occurring of Peierls distortions that may be responsible for the significant loss in discharging capacity.

AUTHOR INFORMATION

Corresponding Author

*(J.L.) Telephone: 086-0574-86688074. E-mail: lijun@nimte.ac.cn.

Notes

The authors declare no competing financial interest.

ACKNOWLEDGMENTS

The authors acknowledge programs supported by the Ningbo Key Innovation Team (2011B82005), the Ningbo postdoctoral Foundation, the National Research program of China (2012CB722700 and SS2013AA050901) and the National Natural Science Foundation of China (11174301, 21303235). Shanghai Supercomputer Center is thanked for providing computation resources. We gratefully acknowledge Guoqiang Liu, Xiaobo Chen, Aicui Wang, Yong Liu, Xianhui Zhang, and Deepak Srivastava for helpful discussions.

REFERENCES

- (1) Thackeray, M. M.; Wolverton, C.; Isaacs, E. D. Electrical Energy Storage for Transportation-Approaching the Limits of, and Going beyond, Lithium-Ion Batteries. *Energy Environ. Sci.* **2012**, *5*, 7854–7863.
- (2) Chebiam, R. V.; Prado, F.; Manthiram, A. Soft Chemistry Synthesis and Characterization of Layered $\text{Li}_{1-x}\text{Ni}_{1-y}\text{Co}_y\text{O}_{2-\delta}$ ($0 \leq x \leq 1$ and $0 \leq y \leq 1$). *Chem. Mater.* **2001**, *13*, 2951–2957.
- (3) Arunkumar, T. A.; Wu, Y.; Manthiram, A. Factors Influencing the Irreversible Oxygen Loss and Reversible Capacity in Layered $\text{Li}[\text{Li}_{1/3}\text{Mn}_{2/3}]\text{O}_2\text{--Li}[\text{M}]\text{O}_2$ ($\text{M} = \text{Mn}_{0.5-y}\text{Ni}_{0.5-y}\text{Co}_{2y}$ and $\text{Ni}_{1-y}\text{Co}_y$) Solid Solutions. *Chem. Mater.* **2007**, *19*, 3067–3073.
- (4) Kang, B.; Ceder, G. Battery Materials for Ultrafast Charging and Discharging. *Nature* **2009**, *458*, 190–193.
- (5) Simon, P.; Gogotsi, Y. Materials for Electrochemical Capacitors. *Nat. Mater.* **2008**, *7*, 845–854.
- (6) Sun, Y.-K.; Myung, S.-T.; Park, B.-C.; Prakash, J.; Belharouak, I.; Amine, K. High-energy Cathode Material for Long-Life and Safe Lithium Batteries. *Nat. Mater.* **2009**, *8*, 320–324.
- (7) Padhi, A. K.; Nanjundaswamy, K. S.; Goodenough, J. B. Phospho-Olivines as Positive-Electrode Materials for Rechargeable Lithium Batteries. *J. Electrochem. Soc.* **1997**, *144*, 1188–1194.
- (8) Goodenough, J. B.; Kim, Y. Challenges for Rechargeable Li Batteries. *Chem. Mater.* **2010**, *22*, 587–603.

- (9) Lee, S. W.; Carlton, C.; Risch, M.; Surendranath, Y.; Chen, S.; Furutsuki, S.; Yamada, A.; Nocera, D. G.; Shao-Horn, Y. The Nature of Lithium Battery Materials under Oxygen Evolution Reaction Conditions. *J. Am. Chem. Soc.* **2012**, *134*, 16959–16962.
- (10) Johannes, M. D.; Hoang, K.; Allen, J. L.; Gaskell, K. Hole Polaron Formation and Migration in Olivine Phosphate Materials. *Phys. Rev. B* **2012**, *85*, 115106–115111.
- (11) Markevich, E.; Sharabi, R.; Haik, O.; Borgel, V.; Salitra, G.; Aurbach, D.; Semrau, G.; Schmidt, M. A.; Schall, N.; Stinner, C. Raman Spectroscopy of Carbon-coated LiCoPO_4 and LiFePO_4 Olivines. *J. Power Sources* **2011**, *196*, 6433–6439.
- (12) Nyten, A.; Abouimrane, A.; Armand, M.; Gustafsson, T.; Thomas, J. O. Electrochemical Performance of $\text{Li}_2\text{FeSiO}_4$ as a New Li-Battery Cathode Material. *Electrochem. Commun.* **2005**, *7*, 156–160.
- (13) Saracibar, A.; Van der Ven, A.; Arroyo-de Dompablo, M. E. Crystal Structure, Energetics, And Electrochemistry of $\text{Li}_2\text{FeSiO}_4$ Polymorphs from First Principles Calculations. *Chem. Mater.* **2012**, *24*, 495–503.
- (14) Eames, C.; Armstrong, A. R.; Bruce, P. G.; Islam, M. S. Insights into Changes in Voltage and Structure of $\text{Li}_2\text{FeSiO}_4$ Polymorphs for Lithium-Ion Batteries. *Chem. Mater.* **2012**, *24*, 2155–2161.
- (15) Santamaria-Perez, D.; Amador, U.; Tortajada, J.; Dominko, R.; Arroyo-de Dompablo, M. E. High-Pressure Investigation of $\text{Li}_2\text{MnSiO}_4$ and $\text{Li}_2\text{CoSiO}_4$ Electrode Materials for Lithium-Ion Batteries. *Inorg. Chem.* **2012**, *51*, 5779–5786.
- (16) Islam, M. S.; Dominko, R.; Masquelier, C.; Sirisopanaporn, C.; Armstrong, A. R.; Bruce, P. G. Silicate Cathodes for Lithium Batteries: Alternatives to Phosphates? *J. Mater. Chem.* **2011**, *21*, 9811–9818.
- (17) Arroyo-deDompablo, M. E.; Dominko, R.; Gallardo-Amores, J. M.; Dupont, L.; Mali, G.; Ehrenberg, H.; Jamnik, J.; Morán, E. On the Energetic Stability and Electrochemistry of $\text{Li}_2\text{MnSiO}_4$ Polymorphs. *Chem. Mater.* **2008**, *20*, 5574–5584.
- (18) Meng, Y. S.; Arroyo-de Dompablo, M. E. Recent Advances in First Principles Computational Research of Cathode Materials for Lithium-Ion Batteries. *Acc. Chem. Res.* **2013**, *46*, 1171–1180.
- (19) Duncan, H.; Kondamreddy, A.; Mercier, P. H. J.; Le Page, Y.; Abu-Lebdeh, Y.; Couillard, M.; Whitfield, P. S.; Davidson, I. J. Novel Pn Polymorph for $\text{Li}_2\text{MnSiO}_4$ and Its Electrochemical Activity As a Cathode Material in Li-Ion Batteries. *Chem. Mater.* **2011**, *23*, 5446–5456.
- (20) Rangappa, D.; Murukanahally, K. D.; Tomai, T.; Unemoto, A.; Honma, I. Ultrathin Nanosheets of Li_2MSiO_4 ($M = \text{Fe, Mn}$) as High-Capacity Li-Ion Battery Electrode. *Nano Lett.* **2012**, *12*, 1146–1151.
- (21) Kempaiah, D. M.; Rangappa, D.; Honma, I. Controlled Synthesis of Nanocrystalline $\text{Li}_2\text{MnSiO}_4$ Particles for High Capacity Cathode Application in Lithium-Ion Batteries. *Chem. Commun.* **2012**, *48*, 2698–2700.
- (22) Gong, Z. L.; Li, Y. X.; Yang, Y. Synthesis and Electrochemical Performance of $\text{Li}_2\text{CoSiO}_4$ as Cathode Material for Lithium ion Batteries. *J. Power Sources* **2007**, *174*, S24–S27.
- (23) Lyness, C.; Delobel, B.; Armstrong, A. R.; Bruce, P. G. The Lithium Intercalation Compound $\text{Li}_2\text{CoSiO}_4$ and Its Behaviour as a Positive Electrode for Lithium Batteries. *Chem. Commun.* **2007**, *46*, 4890–4892.
- (24) Longo, R. C.; Xiong, K.; Cho, K. Multicomponent Silicate Cathode Materials for Rechargeable Li-Ion Batteries: An Ab Initio Study. *J. Electrochem. Soc.* **2013**, *160*, A60–A65.
- (25) Boulineau, A.; Sirisopanaporn, C.; Dominko, R.; Armstrong, A. R.; Bruce, P. G.; Masquelier, C. Polymorphism and structural defects in $\text{Li}_2\text{FeSiO}_4$. *Dalton Trans.* **2010**, *39*, 6310–6316.
- (26) Arroyo-de Dompablo, M. E.; Armand, M.; Tarascon, J. M.; Amador, U. On-Demand Design of Polyoxianionic Cathode Materials Based on Electronegativity Correlations: An Exploration of the Li_2MSiO_4 System ($M = \text{Fe, Mn, Co, Ni}$). *Electrochem. Commun.* **2006**, *8*, 1292–1298.
- (27) Wu, S. Q.; Zhu, Z. Z.; Yang, Y.; Hou, Z. F. Structural Stabilities, Electronic Structures and Lithium Deintercalation in Li_xMSiO_4 ($M = \text{Mn, Fe, Co, Ni}$): A GGA and GGA+U Study. *Comput. Mater. Sci.* **2009**, *44*, 1243–1251.
- (28) Zhong, G.; Li, Y.; Yan, P.; Liu, Z.; Xie, M.; Lin, H. Structural, Electronic, and Electrochemical Properties of Cathode Materials Li_2MSiO_4 ($M = \text{Mn, Fe, and Co}$): Density Functional Calculations. *J. Phys. Chem. C* **2010**, *114*, 3693–3700.
- (29) Zhang, C.; Chen, Z.; Li, J. Ordering Determination of $\text{Li}_2\text{CoSiO}_4$ Polymorphs by First-Principles Calculations. *Chem. Phys. Lett.* **2013**, *580*, 115–119.
- (30) Armstrong, A. R.; Lyness, C.; Menetrier, M.; Bruce, P. G. Structural Polymorphism in $\text{Li}_2\text{CoSiO}_4$ Intercalation Electrodes: A Combined Diffraction and NMR Study. *Chem. Mater.* **2010**, *22*, 1892–1900.
- (31) Kresse, G.; Furthmüller, J. Efficient Iterative Schemes for Ab Initio Total-Energy Calculations Using a Plane-Wave Basis Set. *Phys. Rev. B* **1996**, *54*, 11169–11186.
- (32) Blochl, P. E. Projector Augmented-Wave Method. *Phys. Rev. B* **1994**, *50*, 17953–17979.
- (33) Kresse, G.; Joubert, D. From ultrasoft pseudopotentials to the projector augmented-wave method. *Phys. Rev. B* **1999**, *59*, 1758–1775.
- (34) Perdew, J. P.; Burke, K.; Ernzerhof, M. Generalized Gradient Approximation Made Simple. *Phys. Rev. Lett.* **1996**, *77*, 3865–3868.
- (35) Chevrier, V. L.; Ong, S. P.; Armiento, R.; Chan, M. K. Y.; Ceder, G. Hybrid Density Functional Calculations of Redox Potentials and Formation Energies of Transition Metal Compounds. *Phys. Rev. B* **2010**, *82*, 075122–1–075122–11.
- (36) Zhou, F.; Cococcioni, M.; Marianetti, C. A.; Morgan, D.; Ceder, G. First-Principles Prediction of Redox Potentials in Transition-Metal Compounds with LDA+U. *Phys. Rev. B* **2004**, *70*, 235121–235128.
- (37) Xu, B.; Meng, S. Factors Affecting Li Mobility in Spinel LiMn_2O_4 —A First-Principles Study by GGA and GGA+U Methods. *J. Power Sources* **2010**, *195*, 4971–4976.
- (38) Ceder, G.; Aydinol, M. K.; Kohan, A. F. Application of First-Principles Calculations to the Design of Rechargeable Li-Batteries. *Comput. Mater. Sci.* **1997**, *8*, 161–169.
- (39) Zhou, F.; Cococcioni, M.; Kang, K.; Ceder, G. The Li Intercalation Potential of LiMPO_4 and LiMSiO_4 Olivines with $M = \text{Fe, Mn, Co, Ni}$. *Electrochem. Commun.* **2004**, *6*, 1144–1148.
- (40) Meng, Y. S.; Arroyo-de Dompablo, M. E. First Principles Computational Materials Design for Energy Storage Materials in Lithium Ion Batteries. *Energy Environ. Sci.* **2009**, *2*, 589–609.
- (41) Chen, Z.; Li, J.; Zhang, Z. First Principles Investigation of Electronic Structure Change and Energy Transfer by Redox in Inverse Spinel Cathodes LiNiVO_4 and LiCoVO_4 . *J. Mater. Chem.* **2012**, *22*, 18968–18974.
- (42) Wu, S. Q.; Zhang, J. H.; Zhu, Z. Z.; Yang, Y. Structural and Electronic Properties of the Li-Ion Battery Cathode Material $\text{Li}_x\text{CoSiO}_4$. *Curr. Appl. Phys.* **2007**, *7*, 611–616.
- (43) Sirisopanaporn, C.; Masquelier, C.; Bruce, P. G.; Armstrong, A. R.; Dominko, R. Dependence of $\text{Li}_2\text{FeSiO}_4$ Electrochemistry on Structure. *J. Am. Chem. Soc.* **2010**, *133*, 1263–1265.
- (44) Olalde-Velasco, P.; Jimenez-Mier, J.; Denlinger, J. D.; Hussain, Z.; Yang, W. L. Direct Probe of Mott-Hubbard to Charge-Transfer Insulator Transition and Electronic Structure Evolution in Transition-Metal systems. *Phys. Rev. B* **2011**, *83*, 241102–241105.
- (45) Armand, M.; Tarascon, J. M.; Arroyo-de Dompablo, M. E. Comparative Computational Investigation of N and F Substituted Polyoxoanionic Compounds: The Case of $\text{Li}_2\text{FeSiO}_4$ Electrode Material. *Electrochem. Commun.* **2011**, *13*, 1047–1050.
- (46) Kinyanjui, M. K.; Axmann, P.; Wohlfahrt-Mehrens, M.; Moreau, P.; Boucher, F.; Kaiser, U. Origin of Valence and Core Excitations in LiFePO_4 and FePO_4 . *J. Phys.: Condens. Matter* **2010**, *22*, 275501–275508.